Available online at BCREC website: https://bcrec.id

Bulletin of Chemical Reaction Engineering & Catalysis, 16 (4) 2021, 696-706

Research Article

The Utilization of Mg-Al/Cu as Selective Adsorbent for Cationic Synthetic Dyes

Arini Fousty Badri[1], Neza Rahayu Palapa[1], Risfidian Mohadi[1], M. Mardiyanto[1], Fitri Suryani Arsyad[2], Aldes Lesbani[1,3,*]

[1]Graduate School of Mathematics and Natural Sciences, Universitas Sriwijaya, Jl. Palembang-Prabumulih, Km. 32, Ogan Ilir 30662, South Sumatra, Indonesia.
[2]Department of Physics, Faculty of Mathematics and Natural Sciences, Universitas Sriwijaya, Indonesia.
[3]Research Center of Inorganic Materials and Complexes, Faculty of Mathematics and Natural Sciences, Universitas Sriwijaya, Jl. Padang Selasa Bukit Besar Palembang 30139, South Sumatra, Indonesia.

Received: 21st May 2021; Revised: 23rd July 2021; Accepted: 24th July 2021
Available online: 26th July 2021; Published regularly: December 2021

Abstract

Mg-Al-LDH is a chemical compound produced through co-precipitation technique and modified with $Cu(NO_3)_2.6H_2O$ to form Mg-Al/Cu. However, the research on the capability of these compounds for adsorbing mixtures of cationic dyes as well as malachite green (MG), methylene blue (MB), and Rodhamine-B (Rh-B) has not been carried out. Therefore, this research aims to determine the performance of Mg-Al-LDH and Mg-Al/Cu for removing cationic dyes. The materials used were characterized by using XRD powder, FT-IR, and N_2 adsorption desorption. The Adsorption process was conducted by batch system and several effects were investigated, such as kinetic parameter, isotherm, and the temperature condition. The stability feature of Mg-Al-LDH and Mg-Al/Cu was obtained from the regeneration process in the five cycles. The results presented that Mg-Al/Cu was effectively produced, which was indicated by the formation of layer at 10.792° (003), 22.94° (006), 35.53° (112), 55.78° (110), and 56.59° (116). Mg-Al-LDH and Mg-Al/Cu were found to adsorbed MG than the other cationic dyes with adsorption capacity of 68.996 mg/g and 104.167 mg/g, respectively. The unique properties of Mg-Al/Cu includes, structural stability towards the reuse of adsorbent subsequently for five times, without significant decrease of adsorption capacity.

Keywords: Malachite Green; Layered Double Hydroxide; Mg-Al; Mg-Al/Cu Adsorption

How to Cite: A.F. Badri, N.R. Palapa, R. Mohadi, M. Mardiyanto, F.S. Arsyad, A. Lesbani (2021). The Utilization of Mg-Al/Cu as Selective Adsorbent for Cationic Synthetic Dyes. *Bulletin of Chemical Reaction Engineering & Catalysis*, 16(4), 696-706 (doi:10.9767/bcrec.16.4.11043.696-706)

Permalink/DOI: https://doi.org/10.9767/bcrec.16.4.11043.696-706

1. Introduction

In recent years, dyes are widely utilized for coloring agent in diverse industries, as well as in plastics, rubber, paper, and electroplating manufactory [1–3]. They are also used as additives in food, cosmetics, petroleum products and pharmaceuticals [4,5]. The dyes wastewater endanger the ecosystem of water, because they are difficult to degrade, therefore, decreasing light penetration which further reduces the photosynthetic process of aquatic system [6]. Most dyes are intrinsically toxic and carcinogenic [7]. Therefore, the handling of their disposal has turned out to be a serious issue and need effective treatment [8,9]. Many methods have been researched to remove dyes from aqueous

* Corresponding Author.
Email: aldeslesbani@pps.unsri.ac.id (A. Lesbani);

solution, such as: oxidation [10], membrane separation [11], photodegradation [12], biological process [13], and adsorption [14]. Among all the methods, adsorption is the most effective for removing dyes, because of its easy operation, swift process, and high efficiency [15,16]. Layered double hydroxides (LDHs), generally known as hydrotalcite-like is an inorganic anion-exchangeable adsorbent, used for adsorbing toxic materials from polluted water [17,18].

Research showed that the use of LDH as an adsorbent removes dyes effectively. Shan *et al.* [19] used Mg-Al LDH to remove red dyes with maximum adsorption capacity of 37.16 mg/g for Congo Red and 59.49 mg/g for Reactive Red with optimal adsorbent dosage of 1.0 g and contact time of 60 min. Ouassif *et al.* [20] applied ZnAl LDH for tartrazine dye with adsorption capacity of 99.5 mg/g at pH 5.8 after 60 mins. Ali *et al.* [21] used Ni-Al to remove congo red from aqueous solutions with maximum adsorption capacity of 80.94 mg/g. Grover *et al.* [22] fabricated Zn-Al LDH for brilliant green removal with maximum adsorption capacity of 87.0 mg/g at 15 to 35 °C. Based on these reports, it was observed that the dyes adsorption capacity is still limited, therefore, the modification of LDH need to be conducted widely.

Recently, the LDH modification open a new window research for faster and high rates of removing dyes. In this study, Mg-Al LDH was chosen as the precursor material and was modified with $Cu(NO_3)_2.6H_2O$, in order to enhance the cationic adsorption capacity. MG, MB, and Rh-B are synthetic cationic dyes which are undegradable by microbial in aquatic system, therefore, their removal in these dye are vital. In this research, Copper (Cu) was used as a supporting materials due to its enormous versatility, allowing the expansion of multifunctional materials with some applications, such as: in adsorption, antimicrobial compounds, catalyst, and energy storage [23]. However, the stability of LDH also increased after modification toward reusability adsorbent. The adsorption was conducted by batch system and investigated through the effect of contact time, isotherm fit parameter, and regeneration studies. The structure of MG, MB and Rh-B were shown in Figure 1.

2. Materials and Methods

2.1 Chemical and Characterization

$Mg(NO_3)_2 \cdot 6H_2O$ (400.15 g/mol), $Al(NO_3).9H_2O$ (375.13 g/mol), and $Cu(NO_3)_2.6H_2O$ (290.79 g/mol) were obtained from Sigma-Aldrich. The samples were tested by using X-ray diffraction performed with a Rigaku Miniflex-6000 diffractometer. The surface area where the materials were obtained was measured with a Quantachrome adsorption–desorption. The FTIR spectrum was determined using a Shimadzu Prestige-21 spectrophotometer and the dyes concentration were recorded by using UV-Visible spectrophotometer Biobase BK 1800 at 554 nm for Rh-B, 617 for MG, and 664 for MB.

2.2 Synthesis of Mg-Al-LDH and Mg-Al/Cu

Mg-Al-LDH was produced through co-precipitation method following the procedure in previous research [24]. To obtained Mg/Al-Cu, a mixture of $Mg(NO_3)_2.6H_2O$ with $Al(NO_3).9H_2O$ in the proportion 3:1 of Mg^{2+} and Al^{3+}, and 25 mL $Cu(NO_3)_2.6H_2O$ (0.75 M) were added. The preparation was mixed under vigorous stirring at pH 10. The resulting suspension was heated for 24 h at 80° and dried in oven for 6 h at 250 °C.

2.3 Selectivity of Dyes Mixture

The selectivity was conducted on the adsorbents. As much as 2 mg with 20 mL of dyes (MG, MB, Rh-B) were stirred for several minutes and the contact times was investigated from 10 to 150 min. The dye concentrations were recorded by using UV-Vis spectrophotometer.

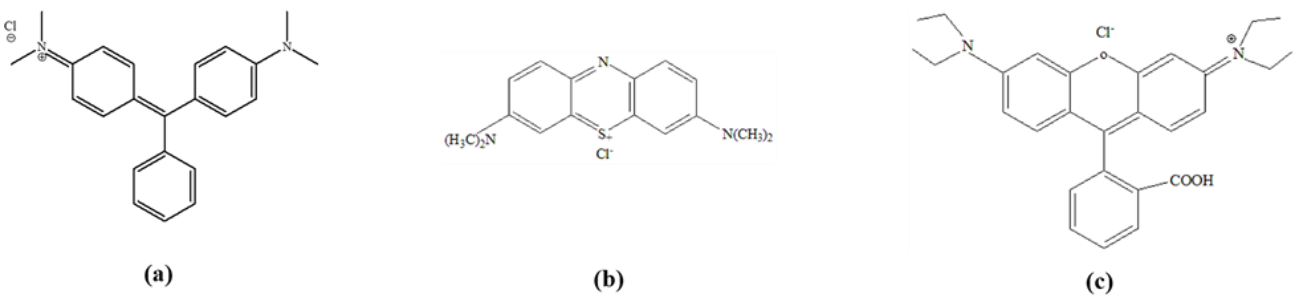

Figure 1. Structure of MG, MB and Rh-B.

2.4 Adsorption Process

After obtaining the most adsorbed dye in the selectivity, the process continued with adsorption by varying the time, concentration, and temperature. The adsorption was conducted for 10–200 min, and the concentration was tested at range of 20–100 ppm and temperature of 303–333 K. The concentration of dye in the filtrate after adsorption was analyzed by using UV-Vis spectrophotometer.

2.4 Regeneration Experiment

As much as 5 g adsorbent were add with 50 mL MG in glass bottle and stirred for 120 min, then dried for 2 h. Then 0.01 g of the residue was added with water and HCl, and stirred for 120 min. This process was repeated in five cycles.

3. Results and Discussion

3.1 Materials and Characterization

The phase structures of the adsorbents were determined from X-ray diffraction pattern and shown in Figure 2. The peak of diffraction on Mg-Al-LDH was indicated at 11.47 ° (003), 22.86° (006), 34.69° (112), 60.33° (110), and 61.62° (116) (JCPDS no. 70-215). Meanwhile, Mg-Al/Cu pattern showed peak at 10.792° (003), 22.94° (006), 35.53° (112), 55.78° (110) and 56.59° (116). Cu oxides at Figure 2b appeared at 29.51 Å and 32 Å with high diffraction peaks. The presence of (003), (006), (112), (110) and (116) planes indicated that the materials were successfully fabricated.

Figure 3 depicts the nitrogen desorption of Mg-Al-LDH and Mg-Al/Cu. Obviously, the two samples presented type IV isotherms, which was classified as H3 hysteresis loop. The material sizes were indicated in the mesoporous nature. The surface area of Mg-Al-LDH after modification was slightly increased from 21.511 m^2/g to 23.139 m^2/g, and was shown in Table 1. Furthermore, diameter pore of Mg-Al/Cu was smaller than the pristine. It was assumed that there were more active sites formed in the modification process.

The spectra obtained in the IR of Mg-Al-LDH in Figure 4 at 3430 cm^{-1}, indicated intense and broad band, which was attributed to stretching vibrations of OH groups of water molecules and the layer. The stretching vibration was board because it was associated with vibration of hydroxyl group in water molecule at 1635 cm^{-1}. The peak at 1381 cm^{-1} was a consequence of the nitrate ion used as a starting material. The vibration of metal-oxygen was observed at 883.25, 671.23, 447.49 and 354.9 cm^{-1}. As shown in FT-IR spectrum of Mg-Al/Cu, the stretching vibration at 447.49 cm^{-1} was ascribed to the bond of Cu–O, which

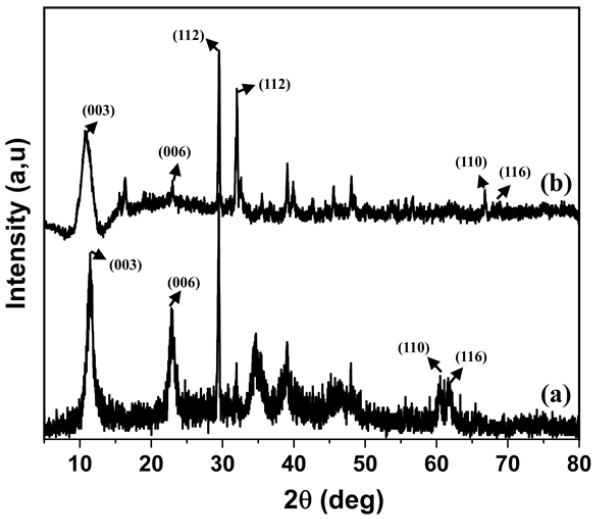

Figure 2. XRD patterns of Mg-Al-LDH (a) and Mg-Al/Cu (b).

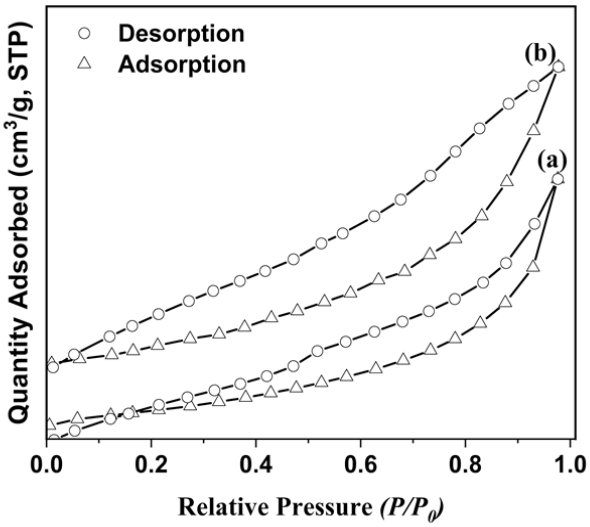

Figure 3. Adsorption and desorption of nitrogen Mg-Al-LDH (a) and Mg-Al/Cu (b).

Table 1. Morphology analysis of LDHs using BET and BJH method.

Adsorbents	Surface Area (m^2/g)	Volume Pore (BJH) (cc/MB)	d-Pore (BJH) (nm)
Mg-Al-LDH	21.511	3.200	6.564
Mg-Al /Cu	23.139	0.067	3.172

confirmed the presence of Mg-Al/Cu. The increasing of the band intensity at 700–500 cm^{-1}, was due to the presence of Cu oxides on the surface of LDH.

The capability of the obtained material as selective adsorbents in a mixture of cationic dyes (MG, MB, and Rh-B), with varied pH were shown in Figure 5. Comparing with MB and Rh-B, Mg-Al/Cu removed MG at contact time range of 10–30 min, and attained an equilibrium at 60–150 min. This is because the size of MG is smaller than MB and Rh-B. Therefore, Mg-Al/Cu showed good adsorption performance and selectivity for removing MG. The dyes concentrations in adsorption selectivity of MG, MB, and Rh-B using Mg-Al/Cu adsorbent was shown on Table 2. The data showed that Mg-Al/Cu was selective on MG, compared to MB and Rh-B with optimum condition without adjustment of pH. MG concentration decreased from 10 mg/L to 5.633 mg/L in 150 minutes. However, at acidic condition (pH 3) and alkaline (pH 9), the concentration of MG decreased from 10 mg/L to 7.132 and 5.840 mg/L, respectively. In previous research, Xu *et al.* [25] reported that pH has an important role in adsorption selectivity. In acidic pH, the dye molecule was protonated and at alkaline it was deprotonated. In previous research of using Zn-Al LDH as an adsorbent, methyl orange was deprotonated at high pH values [26]. In acidic condition, H^+ ion was increased due to decrease in the active adsorption spots on the surface of C-Zn-Al LDH [27].

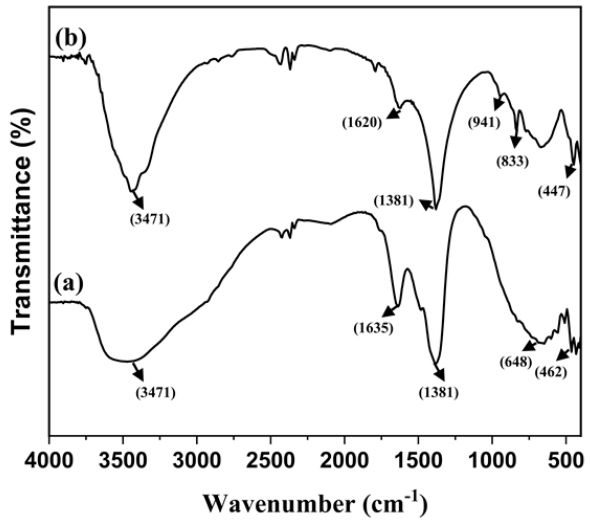

Figure 4. IR Spectra of Mg-Al-LDH (a) and Mg-Al/Cu (b).

3.2 MG Adsorption onto Mg-Al-LDH and Mg-Al/Cu.

The Adsorption of MG on Mg-Al-LDH and Mg-Al/Cu were investigated by kinetic parameter and adsorption isotherms. In this research, the contact time varied from 10–200 min, which was presented by Pseudo First Order

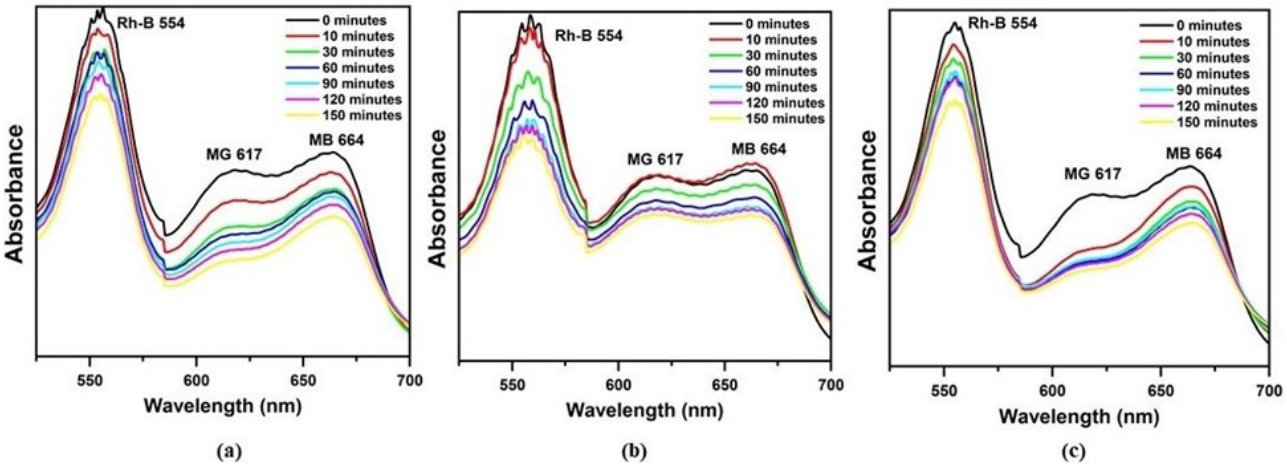

Figure 5. Adsorption selectivity in a mixture of cationic on Mg-Al/Cu, without adjustment of pH (a), pH 3(b), and pH 9 (c).

Table 2. Dyes concentrations in adsorption selectivity using Mg-Al/Cu adsorbent.

times (minutes)	pH	C_o (mg/L)	C_e (mg/L)		
			MB	MG	Rh-B
150	without adjustment pH	10	8.868	5.633	9.237
	3		8.682	7.132	8.778
	9		9.198	5.840	9.300

(PFO) (Equation (1)) and Pseudo Second Order (PSO) (Equation (2)), and the equations were described as follows:

$$\log(q_e - q_t) = \log q_e - \frac{k_1 t}{2.303} \quad (1)$$

$$\frac{t}{q_t} = \frac{1}{k_2 q_e^2} + \frac{1}{q_e} t \quad (2)$$

q_e is dye adsorbed capacity (mg/g), and k is rate constant of PFO and PSO. The influence of contact time was shown in Figure 6, and the result were summarized in Table 3. The adsorption process was increasing rapidly from the initial process, and finally the equilibrium was reached after 120 min. The data showed that MG adsorption followed PSO model because the q_e values and R2 from PSO were higher than the PFO. As reported by Zhou *et al.* [28], the adsorption followed PSO than PFO, which indicated that the diffusion of intraparticle was the rate limiting step.

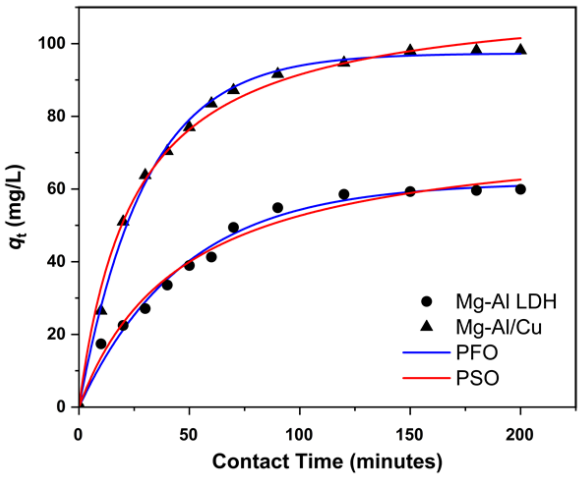

Figure 6. Contact Time variation of MG adsorption on Mg-Al-LDH (a) and Mg-Al/Cu (b).

Figure 7 showed the effect of concentration and temperature variation on MG adsorption. The temperature of MG adsorption was conducted from 303–333 K, with initial concentration of MG at 50–100 mg/L. The MG adsorption was increased sharply from 60 mg/L to 70 mg/L at all temperature, and tend to be stable from 80 mg/L to 100 mg/L after 120 min adsorption. The equations of Langmuir (Equation (3)) and Freundlich (Equation (4)) were presented as follows:

$$\frac{C_e}{q_e} = \frac{1}{q_{max}} C_e + \frac{1}{q_{max} K_L} \quad (3)$$

$$\ln q_e = \ln K_F + \frac{1}{n} \ln C_e \quad (4)$$

where q_{max} and K_L are Langmuir constant, K_F and n are Freundlich constant, with n giving an indication of favorable adsorption process and verifying the type of adsorption process. The MG Adsorption was favorable at high temperature, which was summarized in Table

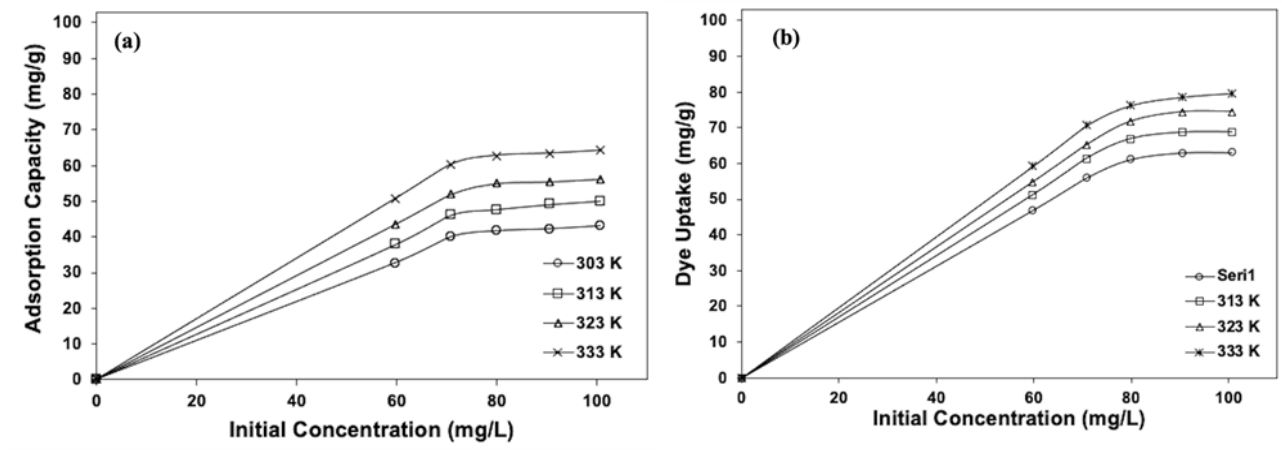

Figure 7. Isotherm fit parameter on MG adsorption into (a) Mg-Al-LDH (b) Mg-Al/Cu.

Table 3. PSO and PFO parameters of MG adsorption onto Mg-Al-LDH (a) and Mg-Al/Cu (b).

Materials	$Q_{e_{exp}}$ (mg/g)	PFO			PSO		
		$Q_{e_{Calc}}$ (mg/g)	R^2	k_1	$Q_{e_{Calc}}$ (mg/g)	R^2	k_2
Mg-Al-LDH	59.938	77.678	0.982	0.031	67.568	0.989	0.0003
Mg-Al/Cu	98.120	77.535	0.974	0.028	106.383	0.998	0.0006

4 and 5, in order to obtain isotherm and thermodynamic parameters.

These data showed that the adsorption of MG on Mg-Al-LDH and Mg-Al/Cu were fitted into Langmuir isotherm model than the Freundlich. The R^2 value for both adsorbents was closer to the Langmuir than Freundlich model. Based on the Langmuir model, the adsorption form a monolayer of dye molecules, because when dyes were adsorbed, the site becomes saturated and unavailable for other molecules [29]. The adsorption capacity of Mg-Al/Cu is higher than the precursor. According to Maziarz *et al*. [30], the phenomena due to the adsorption of the undissolved metal oxide and the mechanism of MG removal, was effected by anion exchange in the interlayer space. It was also affected by the amount of surface area, where Mg/Al-Cu has bigger surface area than Mg/Al The thermodynamic parameter, such as enthalpy (ΔH), entropy (ΔS), and Gibbs energy (ΔG) were calculated using this equation, where T is temperature and R is the gas constant [31].

$$\ln K_L = \frac{\Delta S}{R} - \frac{\Delta H}{RT} \quad (5)$$

$$\Delta G° = \Delta H - T\Delta S \quad (6)$$

The thermodynamic data as shown in Table 5 was also correlated with the adsorption energy, which was dominated by physical adsorption. The adsorption energy for Mg-Al LDH (15.993 kJ/mol) and Mg-Al/Cu (26.715 kJ/mol) were in the range of physical adsorption process and the differences of IR and XRD characterization before and after adsorption process at Figure 8 and Figure 9 indicated of chemisorption processes. The adsorption of MG using Mg/Al-Cu involves both physisorption and chemisorption processes. As the previous research Elkhider *et al.* [32] reported that MO re-

Table 4. Langmuir and Freundlich models of MG adsorption into Mg-Al-LDH and Mg-Al/Cu.

Adsorbent	Adsorption isotherm	Adsorption constant	T (K)			
			303	313	323	333
Mg-Al	Langmuir	Q_{max}	55.556	65.359	67.114	68.966
		K_L	0.066	0.028	0.230	0.115
		R^2	0.8214	0.9523	0.9318	0.9201
	Freundlich	N	1.027	0.682	0.692	0.737
		K_f	3.087	1.615	1.670	1.779
		R^2	0.7225	0.412	0.3563	0.4021
Mg-Al/Cu	Langmuir	Q_{max}	86.027	99.010	103.093	104.167
		K_L	0.073	0.094	0.096	0.038
		R_2	0.9669	0.9702	0.9591	0.9104
	Freundlich	N	0.8273	0.761	0.753	0.760
		K_f	2.4038	2.390	2.408	2.473
		R^2	0.8468	0.9055	0.9133	0.8659

Table 5. Thermodynamic adsorption parameter of MG into Mg-Al-LDH and Mg-Al/CuLDHs.

Adsorbent	T (K)	Q_e (mg/g)	ΔH (kJ/mol)	ΔS (J/mol.K)	ΔG (kJ/mol)
Mg-Al-LDH	303	56.687	15.933	0.048	−1.192
	313	60.847			−1.759
	323	65.008			−2.327
	333	68.398			−2.894
Mg-Al/Cu	303	71.630	26.715	0.099	−3.309
	313	75.821			−4.299
	323	79.119			−5.290
	333	82.262			−6.281

moval onto SF-B-CoNiAl composite was physical adsorption and chemisorption processes, the physisorption was observed form the amount of ΔH (2–40 kJ/mol) and chemisorption was indicated from the kinetic data which followed by pseudo-second order (R^2>0.99). According to Chebli *et al.* [33] the enthalpy values (14.49 kJ/mol) of Biebrich Scarlet (BS) adsorption ascribed that the interaction type is a physical adsorption and the BS adsorption was also followed by chemical adsorption due to the the dye interaction in the interlayer space of the LDHs which shown from the FTIR characterization.

The positive value ΔH reflected that the MG adsorption was endothermic. Moreover, the negative amount of ΔG denoted that MG adsorption was running spontaneous. The endothermic process with negative amount of ΔG indicated that the adsorption was running spontaneous at higher temperatures [34]. The same phenomena also occurred by other research, by using Zn/Al LDH removing MG with ΔH= 14.503 kJ/mol indicated endothermic process and ΔG= −13.513 kJ/mol denoted the adsorption was running spontaneous [35]. According to Palapa *et al.* [36], ΔH and ΔG with the liquid phase were affected by various conditions such as concentration, temperature, and interaction between solid and liquid interfaces. Table 6 showed the comparison of the other adsorbents on MG adsorption.

The IR spectra of Mg-Al/Cu adsorbent after the adsorbed MG was showed on Figure 8. The strong bond of hydroxyl group of water was detected at 3441 cm^{-1} before and 3444 cm^{-1} after MG adsorption. The peak at 1381 cm^{-1} before adsorption process was due to the presence of nitrate ion and was detected at 1361 cm^{-1} after adsorption. The vibration of metal-oxygen was

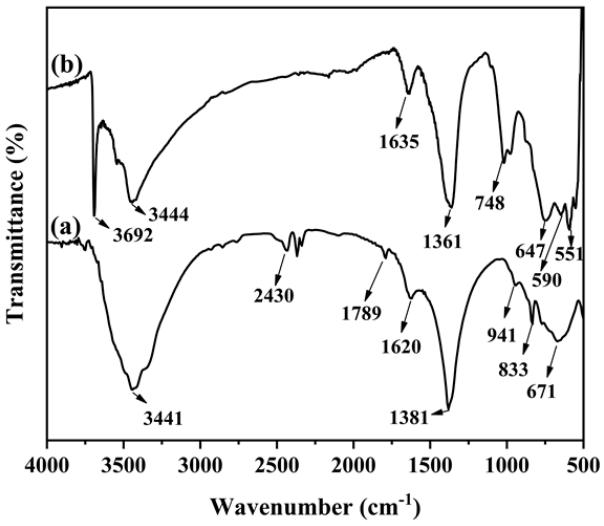

Figure 8. IR Spectra of Mg-Al/Cu before (a) and after (b) MG adsorption.

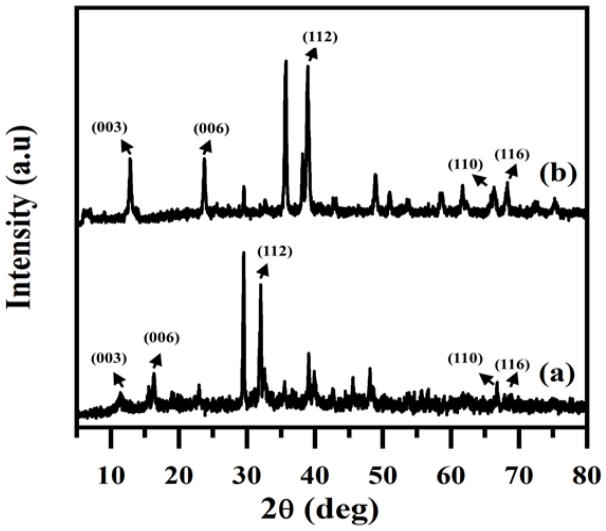

Figure 9. XRD of Mg-Al/Cu before (a) and after (b) MG adsorption.

Table 6. Comparison of MG adsorption capacity with other adsorbents.

Adsorbent	Adsorption Capacity (mg/g)	References
Trichoderma Biomass	81.82	[37]
Cortaderia selloana	56.50	[38]
MWCNT-COOH	11.73	[39]
Date pits	64.7	[40]
Thiolated Graphene Oxide	40.5	[41]
ZnO-NR-AC	20	[42]
Luffa aegayptica peel	70.21	[43]
Ni/Fe LDH	6.93	[44]
Co/Fe LDH	44.73	[45]
Zn/Al LDH	60.7	[46]
Mg/Al LDH	68.996	This Study
Mg-Al/Cu	104.167	This Study

observed at 883.25, 671.23, 447.49 and 354.9 cm^{-1} before adsorption. And also at 748, 647, 551 and 590 cm^{-1} after adsorption.

The XRD of Mg-Al/Cu before and after adsorption was showed in Figure 9. There was visible differences in the diffraction pattern of Mg-Al/Cu before and after MG adsorption. The XRD pattern of Mg-Al/Cu before adsorption showed peak at 10.79° (003), 22.94° (006), 35.53° (112), 55.78° (110), and 56.59° (116). After adsorption, the presence of the diffraction peaks appeared at 12.78°, 24.52°, 38.21°, 66.36°, and 68.30°, which corresponded to the (003), (006), (112), (110), and (116) planes. Mg-Al/Cu characterization for IR and XRD after adsorption showed differences, compared to before the process, which indicated the reaction between adsorbate and adsorbent. As reported in previous research, Mg-Al LDH successfully removed methyl orange, because of the hydrogen bonding that formed and the electrostatic interaction between the reacting entities [47]

The regeneration process was conducted to determine the stability structure of the adsorbents. The regeneration of MG on Mg-Al-LDH and Mg-Al/Cu were shown in Figure 10. At the 1st, 2nd, 3rd, 4th, and 5th cycle, the MG adsorption of Mg-Al LDH was observed at 66.07%, 63.02%, 37.66%, 21.47%, and 7.46%, respectively. Meanwhile, for Mg-Al/Cu, the adsorption of MG reached 82.55%, 76.26%, 64.92%, 54.51%, and 47.28%, at 1st, 2nd, 3rd, 4th, and 5th cycle, respectively. The data showed that MG adsorption process of Mg-Al/Cu was more stable than the pristine compound, after the five cycles. This was because the Mg-Al/Cu surface area and interlayer space was higher than that of Mg-Al LDH. Therefore, the structure of Mg-Al/Cu was stable and the adsorption capacity did not change significantly over the five adsorption cycles.

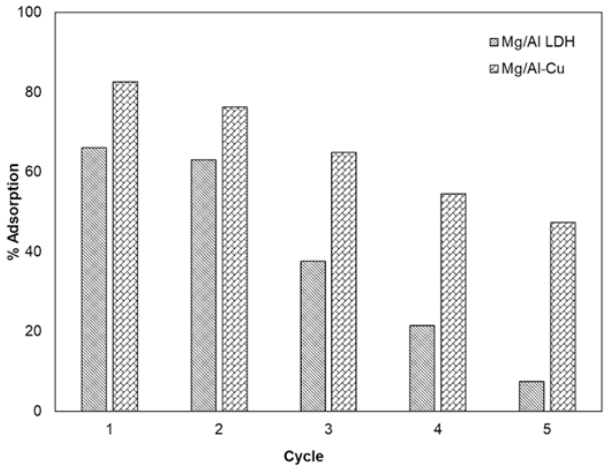

Figure 10. Regeneration of MG on on Mg-Al LDH and Mg-Al/Cu.

4. Conclusion

In conclusion, Mg-Al/Cu was successfully synthesized with well-known layer structure as represented in the XRD, IR and BET characterization. The adsorption of MG on both adsorbents followed PSO kinetic model. The energy of 15.993 kJ/mol for Mg-Al LDH and 26.715 kJ/mol for Mg-Al/Cu was indicated in the physical adsorption process. After five cycles adsorption process, Mg-Al/Cu was found to be more stable than Mg-Al/LDH.

Acknowledgement

The authors are grateful for the financial support granted by Hibah Disertasi Doktor Dikti contract number 150/E4.1/AK.04.PT/2021 and derivative contract number 0166/UN9/SB3.LP2M.PT/2021. Author also thankful to the Research Center of Inorganic Materials and Complexes FMIPA Universitas Sriwijaya for their contribution with instrumental analysis and laboratory facilities.

References

[1] Karami, Z., Jouyandeh, M., Ali, J.A., Ganjali, M.R., Aghazadeh, M., Maadani, M., Rallini, M., Luzi, F., Torre, L., Puglia, D., Akbari, V., Saeb, M.R. (2019). Cure Index for labeling curing potential of epoxy/LDH nanocomposites: A case study on nitrate anion intercalated Ni-Al-LDH. *Progress in Organic Coatings*, 136, 105228. DOI: 10.1016/j.porgcoat.2019.105228

[2] Zhao, G., Liu, L., Li, C., Zhang, T., Yan, T., Yu, J., Jiang, X., Jiao, F. (2018). Construction of diatomite/ZnFe layered double hydroxides hybrid composites for enhanced photocatalytic degradation of organic pollutants. *Journal of Photochemistry and Photobiology A: Chemistry*, 367, 302–311. DOI: 10.1016/j.jphotochem.2018.08.048

[3] Xu, M., Bi, B., Xu, B., Sun, Z., Xu, L. (2018). Polyoxometalate-intercalated ZnAlFe-layered double hydroxides for adsorbing removal and photocatalytic degradation of cationic dye. *Applied Clay Science*, 157, 86–91. DOI: 10.1016/j.clay.2018.02.023

[4] Vinsiah, R., Mohadi, R., Lesbani, A. (2017). Performance of Graphite for Congo Red and Direct Orange Adsorption. *Indonesian Journal of Environmental Management and Sustainability*, 4(4), 125–113. DOI: 10.26554/ijems.2020.4.4.125-132.

[5] Hidayati, N., Mohadi, R., Elfita, E., Lesbani, A. (2020). Malachite Green Removal by Zn/Al-citrate LDHs in Aqueous Solution. *Science and Technology Indonesia*, 5, 59–61. DOI: 10.26554/sti.2020.5.2.59-61

[6] Islam, M.A., Ali, I., Karim, S.M.A., Hossain Firoz, M.S., Chowdhury, A.N., Morton, D.W., Angove, M.J. (2019). Removal of dye from polluted water using novel nano manganese oxide-based materials. *Journal of Water Process Engineering*, 32, 100911. DOI: 10.1016/j.jwpe.2019.100911

[7] Ruan, X., Chen, Y., Chen, H., Qian, G., Frost, R.L. (2016). Sorption behavior of methyl orange from aqueous solution on organic matter and reduced graphene oxides modified Ni-Cr layered double hydroxides. *Chemical Engineering Journal*, 297, 295–303. DOI: 10.1016/j.cej.2016.01.041

[8] Siregar, P.M.S.B.N., Palapa, N.R., Wijaya, A., Fitri, E.S., Lesbani, A. (2021). Structural stability of Ni/Al layered double hydroxide supported on graphite and biochar toward adsorption of congo red. Science and Technology Indonesia, 6(2), 85-95. DOI: 10.26554/sti.2021.6.2.85-95

[9] Oktriyanti, M., Palapa, N.R., Mohadi, R., Lesbani, A. (2019). Modification Of Zn-Cr Layered Double Hydroxide With Keggin Ion. *Indonesian Journal of Environmental Management and Sustainability*, 3, 93–99. DOI: 10.26554/ijems.2019.3.3.93-99

[10] Kang, Y.G., Yoon, H., Lee, C.S., Kim, E.J., Chang, Y.S. (2019). Advanced oxidation and adsorptive bubble separation of dyes using MnO2-coated Fe3O4 nanocomposite. *Water Research*, 151, 413–422. DOI: 10.1016/j.watres.2018.12.038

[11] Xu, Y., Li, Z., Su, K., Fan, T., Cao, L. (2018). Mussel-inspired modification of PPS membrane to separate and remove the dyes from the wastewater. *Chemical Engineering Journal*, 341, 371–382. DOI: 10.1016/j.cej.2018.02.048

[12] Wang, Y., Jiang, F., Chen, J., Sun, X., Xian, T., Yang, H. (2020). In situ construction of CNT/cus hybrids and their application in photodegradation for removing organic dyes. *Nanomaterials*, 10(1), 178. DOI: 10.3390/nano10010178

[13] Popli, S., Patel, U.D. (2015). Destruction of azo dyes by anaerobic–aerobic sequential biological treatment: a review. *International Journal of Environmental Science and Technology*, 12, 405–420. DOI: 10.1007/s13762-014-0499-x

[14] Huang, Q., Song, S., Chen, Z., Hu, B., Chen, J., Wang, X. (2019). Biochar-based materials and their applications in removal of organic contaminants from wastewater: state-of-the-art review. *Biochar*, 1, 45–73. DOI: 10.1007/s42773-019-00006-5

[15] Badri, A.F., Mohadi, R., Lesbani, A. (2021). Adsorptive capacity of malachite green onto Mg/M^{3+} (M^{3+}=Al and Cr) LDHs. *Global NEST Journal*, 23, 1–8. DOI: 10.30955/gnj.003443

[16] Mohadi, R., Palapa, N.R., Lesbani, A. (2021). Preparation of Ca/Al-Layered Double Hydroxides/Biochar Composite with High Adsorption Capacity and Selectivity toward Cationic Dyes in Aqueous. *Bulletin of Chemical Reaction Engineering & Catalysis*, 16, 244–252. DOI: 10.9767/bcrec.16.2.10211.244-252

[17] Taher, T., Christina, M.M., Said, M., Hidayati, N., Ferlinahayati, F., Lesbani, A. (2019). Removal of iron(II) using intercalated Ca/Al layered double hydroxides with [-SiW12O40]4-. *Bulletin of Chemical Reaction Engineering & Catalysis*, 14, 260–267. DOI: 10.9767/bcrec.14.2.2880.260-267

[18] Mohadi, R., Hanafiah, Z., Hermansyah, H., Zulkifli, H. (2017). Adsorption of procion red and congo red dyes using microalgae Spirulina sp. *Science and Technology Indonesia*, 2, 102–104. DOI: 10.26554/sti.2017.2.4.102-104

[19] Shan, R.-r., Yan, L.-g., Yang, Y.-m., Yang, K., Yu, S.-j., Yu, H.-q., Zhu, B.-c., Du, B. (2015). Highly efficient removal of three red dyes by adsorption onto Mg-Al-layered double hydroxide. *Journal of Industrial and Engineering Chemistry*, 21, 561–568. DOI: 10.1016/j.jiec.2014.03.019

[20] Ouassif, H., Moujahid, E.M., Lahkale, R., Sadik, R., Bouragba, F.Z., Sabbar, E.M., Diouri, M. (2020). Zinc-Aluminum layered double hydroxide: High efficient removal by adsorption of tartrazine dye from aqueous solution. *Surfaces and Interfaces*, 18, 100401. DOI: 10.1016/j.surfin.2019.100401

[21] Ali, B., Naceur, B., Abdelkader, E., Karima, E. (2020). Competitive adsorption of binary dye from aqueous solutions using calcined layered double hydroxides. *International Journal of Environmental Analytical Chemistry*, 100, 1–20. DOI: 10.1080/03067319.2020.1766035

[22] Grover, A., Mohiuddin, I., Malik, A.K., Aulakh, J.S., Kim, K.-H. (2019). Zn-Al layered double hydroxides intercalated with surfactant: Synthesis and applications for efficient removal of organic dyes. *Journal of Cleaner Production*, 240, 118090. DOI: 10.1016/j.jclepro.2019.118090

[23] Berner, S., Araya, P., Govan, J., Palza, H. (2018). Cu/Al and Cu/Cr based layered double hydroxide nanoparticles as adsorption materials for water treatment. *Journal of Industrial and Engineering Chemistry*, 59, 134–140. DOI: 10.1016/j.jiec.2017.10.016

[24] Badri, A.F., Siregar, P.M.S.B.N., Palapa, N.R., Mohadi, R., Mardiyanto, M., Lesbani, A. (2021). Mg-Al/Biochar Composite with Stable Structure for Malachite Green Adsorption from Aqueous Solutions. *Bulletin of Chemical Reaction Engineering & Catalysis*, 16, 149–160. DOI: 10.9767/bcrec.16.1.10270.149-160

[25] Xu, H., Zhu, S., Xia, M., Wang, F. (2021). Rapid and efficient removal of diclofenac sodium from aqueous solution via ternary core-shell CS@PANI@LDH composite: Experimental and adsorption mechanism study. *Journal of Hazardous Materials*, 402, 123815. DOI: 10.1016/j.jhazmat.2020.123815

[26] Mahjoubi, F.Z., Elhalil, A., Elmoubarki, R., Sadiq, M., Khalidi, A., Cherkaoui, O., Barka, N. (2017). Performance of Zn-, Mg- and Ni-Al layered double hydroxides in treating an industrial textile wastewater. *Journal of Applied Surfaces and Interfaces*, 2, 1–11. DOI: 10.48442/IMIST.PRSM/jasi-v2i1-3.10033.

[27] George, G., Saravanakumar, M.P. (2018). Facile synthesis of carbon-coated layered double hydroxide and its comparative characterisation with Zn–Al LDH: application on crystal violet and malachite green dye adsorption—isotherm, kinetics and Box-Behnken design. *Environmental Science and Pollution Research*, 25, 30236–30254. DOI: 10.1007/s11356-018-3001-3

[28] Zhou, H., Jiang, Z., Wei, S. (2018). A new hydrotalcite-like absorbent FeMnMg-LDH and its adsorption capacity for Pb2+ ions in water. *Applied Clay Science*, 153, 29–37. DOI: 10.1016/j.clay.2017.11.033

[29] Lafi, R., Charradi, K., Djebbi, M.A., Ben Haj Amara, A., Hafiane, A. (2016). Adsorption study of Congo red dye from aqueous solution to Mg-Al-layered double hydroxide. *Advanced Powder Technology*, 27, 232–237. DOI: 10.1016/j.apt.2015.12.004

[30] Maziarz, P., Matusik, J., Strączek, T., Kapusta, C., Woch, W.M., Tokarz, W., Radziszewska, A., Leiviskä, T. (2019). Highly effective magnet-responsive LDH-Fe oxide composite adsorbents for As(V) removal. *Chemical Engineering Journal*, 362, 207–216. DOI: 10.1016/j.cej.2019.01.017

[31] Elmoubarki, R., Mahjoubi, F.Z., Elhalil, A., Tounsadi, H., Abdennouri, M., Sadiq, M., Qourzal, S., Zouhri, A., Barka, N. (2017). Ni/Fe and Mg/Fe Layered Double Hydroxides and Their Calcined Derivatives: Preparation, Characterization and Application on Textile Dyes Removal. *Journal of Materials Research and Technology*, 6, 271–283. DOI: 10.1016/j.jmrt.2016.09.007

[32] Elkhider, K.H.A., Ihsanullah, I., Zubair, M., Manzar, M.S., Mu'azu, N.D., Al-Harthi, M.A. (2020). Synthesis, Characterization and Dye Adsorption Performance of Strontium Ferrite decorated Bentonite-CoNiAl Magnetic Composite. *Arabian Journal for Science and Engineering*, 45, 7397–7408. DOI: 10.1007/s13369-020-04544-0

[33] Chebli, D., Bouguettoucha, A., Reffas, A., Tiar, C., Boutahala, M., Gulyas, H., Amrane, A. (2016). Removal of the anionic dye Biebrich scarlet from water by adsorption to calcined and non-calcined Mg–Al layered double hydroxides. *Desalination and Water Treatment*, 57, 22061–22073. DOI: 10.1080/19443994.2015.1128365

[34] Muangthong-On, T., Wannapeera, J., Ohgaki, H., Miura, K. (2017). TG-DSC Study to Measure Heat of Desorption of Water during the Thermal Drying of Coal and to Examine the Role of Adsorption of Water Vapor for Examining Spontaneous Heating of Coal over 100 °c. *Energy and Fuels*, 31, 10691–10698. DOI: 10.1021/acs.energyfuels.7b01836

[35] George, G., Saravanakumar, M.P. (2018). Facile synthesis of carbon-coated layered double hydroxide and its comparative characterisation with Zn–Al LDH: application on crystal violet and malachite green dye adsorption—isotherm, kinetics and Box-Behnken design. *Environmental Science and Pollution Research*, 25, 30236–30254. DOI: 10.1007/s11356-018-3001-3

[36] Palapa, N.R., Juleanti, N., Normah, N., Mohadi, R., Taher, T., Rachmat, A., Lesbani, A. (2020). Copper Aluminum Layered Double Hydroxide Modified by Biochar and its Application as an Adsorbent for Procion Red. *Journal of Water and Environment Technology*, 18, 359–371. DOI: 10.2965/JWET.20-059

[37] Argumedo-Delira, R., Gómez-Martínez, M.J., Uribe-Kaffure, R. (2021). Trichoderma biomass as an alternative for removal of congo red and malachite green industrial dyes. *Applied Sciences*, 11(1), 448. DOI: 10.3390/app11010448

[38] Parlayıcı, Ş., Pehlivan, E. (2021). Biosorption of methylene blue and malachite green on biodegradable magnetic Cortaderia selloana flower spikes: modeling and equilibrium study. *International Journal of Phytoremediation*, 23, 26–40. DOI: 10.1080/15226514.2020.1788502

[39] Rajabi, M., Mirza, B., Mahanpoor, K., Mirjalili, M., Najafi, F., Moradi, O., Sadegh, H., Shahryari-ghoshekandi, R., Asif, M., Tyagi, I., Agarwal, S., Gupta, V.K. (2016). Adsorption of malachite green from aqueous solution by carboxylate group functionalized multi-walled carbon nanotubes: Determination of equilibrium and kinetics parameters. *Journal of Industrial and Engineering Chemistry*, 34, 130–138. DOI: 10.1016/j.jiec.2015.11.001

[40] Hijab, M., Saleem, J., Parthasarathy, P., Mackey, H.R., McKay, G. (2021). Two-stage optimisation for malachite green removal using activated date pits. *Biomass Conversion and Biorefinery*, 11, 727–740. DOI: 10.1007/s13399-020-00813-y

[41] Salamat, S., Mohammadnia, E., Hadavifar, M. (2021). K inetics and Adsorption Investigation of Malachite Green onto Thiolated Graphene Oxide Nanostructures. *Journal of Water and Wastewater*, 31(6), 1–11. DOI: 10.22093/wwj.2020.208052.2951

[42] Azad, F.N., Ghaedi, M., Dashtian, K., Hajati, S., Goudarzi, A., Jamshidi, M. (2015). Enhanced simultaneous removal of malachite green and safranin O by ZnO nanorod-loaded activated carbon: Modeling, optimization and adsorption isotherms. *New Journal of Chemistry*, 39, 7998–8005. DOI: 10.1039/c5nj01281c

[43] Mashkoor, F., Nasar, A. (2019). Preparation, characterization and adsorption studies of the chemically modified Luffa aegyptica peel as a potential adsorbent for the removal of malachite green from aqueous solution. *Journal of Molecular Liquids*, 274, 315–327. DOI: 10.1016/j.molliq.2018.10.119

[44] Lesbani, A., Taher, T., Palapa, N.R., Mohadi, R., Rachmat, A., Mardiyanto. (2020). Preparation and utilization of Keggin-type polyoxometalate intercalated Ni–Fe layered double hydroxides for enhanced adsorptive removal of cationic dye. *SN Applied Sciences*, 2, 4–7. DOI: 10.1007/s42452-020-2300-8

[45] Amin, R.M., Taha, M., Abdel Moaty, S.A., Abo El-Ela, F.I., Nassar, H.F., Gadelhak, Y., Mahmoud, R.K. (2019). Gamma radiation as a green method to enhance the dielectric behaviour, magnetization, antibacterial activity and dye removal capacity of Co-Fe LDH nanosheets. *RSC Advances*, 9, 32544–32561. DOI: 10.1039/c9ra06509a

[46] Mahmoud, R.K., Kotp, A.A., El-Deen, A.G.A., Farghali, A., Abo El-Ela, F.I. (2020). Novel and Effective Zn-Al-GA LDH Anchored on Nanofibers for High-Performance Heavy Metal Removal and Organic Decontamination: Bioremediation Approach. *Water, Air, and Soil Pollution*, 231, 363. DOI: 10.1007/s11270-020-04629-4

[47] Daud, M., Hai, A., Banat, F., Wazir, M.B., Habib, M., Bharath, G., Al-Harthi, M.A. (2019). A review on the recent advances, challenges and future aspect of layered double hydroxides (LDH)– Containing hybrids as promising adsorbents for dyes removal. *Journal of Molecular Liquids*, 288, 110989. DOI: 10.1016/j.molliq.2019.110989